IVYSPRING INTERNATIONAL PUBLISHER

Theranostics

2016; 6(13): 2337-2351. doi: 10.7150/thno.14937

Research Paper

NIR-Laser-Controlled Drug Release from DOX/IR-780-Loaded Temperature-Sensitive-Liposomes for Chemo-Photothermal Synergistic Tumor Therapy

Fei Yan [1,3*], Wanlu Duan [2*], Yekuo Li [2✉], Hao Wu [3], Yuli Zhou [4], Min Pan [1], Hongmei Liu [3], Xin Liu [1] and Hairong Zheng [1,3,5✉]

1. Paul C. Lauterbur Research Center for Biomedical Imaging, Institute of biomedical and Health Engineering, Shenzhen Institutes of Advanced Technology, Chinese Academy of Sciences, Shenzhen, China;
2. Department of Ultrasound, Guangzhou General Hospital of Guangzhou Military Command, Guangzhou, China;
3. Department of Ultrasonography, The Third Affiliated Hospital of Southern Medical University (Academy of Orthopedics Guangdong Province), Guangzhou, China;
4. Department of Ultrasonography, Shenzhen People's Hospital & Second Clinical Medical College of Jinan University, Shenzhen, China;
5. Shenzhen Key Laboratory of Nanobiomechanics, Shenzhen Institutes of Advanced Technology, Chinese Academy of Sciences, Shenzhen, China.

*Both authors contributed equally to this paper.

✉ Corresponding authors: Hairong Zheng and Yekuo Li, E-mails: hr.zheng@siat.ac.cn and yekuoli@163.com Tel.: +86 755 86392284, Fax: +86 755 96382299.

Received: 2016.01.11; Accepted: 2016.05.18; Published: 2016.10.01

Abstract

NIR laser-induced photothermal therapy (PTT) through near-infrared agents has demonstrated the great potential in solid tumor ablation. However, the nonuniform heat distribution over tumors from PTT makes it insufficient to kill all tumor cells, resulting in tumor recurrence and inferior outcomes. To improve the tumor treatment efficacy, it is highly desirable to develop the combinational treatment of PTT with other modalities, especially with chemotherapeutic agents. Here we report a smart DOX/IR-780-loaded temperature-sensitive-liposome (DITSL) which can achieve NIR-laser-controlled drug release for chemo-photothermal synergistic tumor therapy. In this system, the liposoluble IR-780 was incorporated into the temperature-sensitive lipid bilayer and the soluble chemotherapeutic doxorubicin (DOX) was encapsulated in the hydrophilic core. The resulting DITSL is proved to be physiologically stable and can provide a fast and laser irradiation-controllable DOX release in the PBS and cellular conditions. We further employed this nanoparticle for tumor treatment, demonstrating significantly higher tumor inhibition efficacy than that of DOX-loaded temperature-sensitive-liposome (DTSL) or IR780-loaded temperature-sensitive-liposome (ITSL) in the in vitro cells and in vivo animals. Histological analysis further revealed much more apoptotic cells, confirming the advantageous anti-tumor effect of DITSL over DTSL or ITSL. Our study provides a promising strategy to realize chemo-photothermal synergistic combination therapy for breast tumors.

Key words: Photothermal therapy, Temperature-sensitive-liposome, IR-780, Doxorubicin, Breast tumors.

Introduction

Photothermal therapy (PTT) is an attractive technique for solid tumor ablation, by which light energy absorbed by near-infrared (NIR) photothermal agents can convert into thermal energy and produce local hyperthermia, ultimately leading to irreversible cell injury (tumor apoptosis and coagulative necrosis) [1]. NIR laser-induced PTT offers several obvious advantages, including the minimized invasiveness, increased preservation of surrounding tissues, the short recovery times and the reduced complication rates, as well as intra-procedural monitoring by visualization [2]. However, the nonuniform heat

distribution over tumors makes it insufficient to kill all tumor cells, resulting in incomplete ablation, tumor recurrence and inferior outcomes [3]. Therefore, the combined treatments are required to further improve the therapeutic efficacy from NIR-PTT.

To date, there are various combined treatment approaches were developed [4-10]. Among them, the combination of PTT and chemotherapeutic agents shows the most promising prospect to optimize cancer therapy [5, 11-13]. PTT and chemotherapeutic drugs have quite different mechanisms of action. The former mainly ascribes to hyperthermia and may be consider a physical treatment modality. NIR-light in the wavelength range from 700 to 1100 nm can efficiently penetrate into biological tissues and selectively heat PTT agents [14]. This heat produced from laser irradiation can increase the tumor temperature to cause irreversible cellular damage. The latter, a chemotherapy modality, is one of the most commonly therapeutic approach for the treatment of a wide variety of cancers. Since heat is independently cytotoxic, hyperthermia combined with chemotherapeutic drugs often results in superadditive or synergistic effects [15].

Nanoparticle-based nanotechnology provides an effective platform to combine hyperthermia with chemotherapeutic drugs, permitting the design of nano-drugs for targeted heat and drug delivery. Recently, several multifunctional nano-platforms, including hollow gold nanocages and nanospheres [16, 17], CuS nanocages [18], silica-coated nanoparticles [19], were developed for the combination of chemotherapy and photothermal therapy. Although synergistic effects of these systems have been demonstrated in their in-vitro and in-vivo studies, the common drawbacks of these nanomaterials are obvious. Most of them had a temperature-insensitive shell. The drugs were released only after the hard shells were destructed at a relatively high temperature (> 50 °C). Tumor cells, especially those located in the peripheral or transitional zone at temperatures between 41 °C and 45 °C, may not be exposed to enough drug concentrations to kill them [20]. Besides, too high temperature may inactivate certain drugs before their escaping from these destructed shells. A controllable drug release still fails to be well realized by ex-vivo NIR laser. Therefore, the development of smart nanosystems to achieve temperature-controllable and fast drug release is extremely desirable for the combination of chemotherapy and photothermal therapy.

Temperature-sensitive liposomes (TSL) are an especially attractive option since they can release their contents around the physiological temperature. Upon laser-induced heat to 42 °C, the outer membrane of these liposomes undergo a phase transition and become permeable. The encapsulated drug molecules are fast released into the environment in temperature-sensitive manner [21, 22]. When hyperthermia alone is not sufficient to induce complete tumor eradication, the temperature elevation is still sufficient to cause a phase transition of TSL and to increase drug release within tumors [23]. In recent years, some studies which used TSL as carriers to encapsulate different chemo-drugs and heat-generation materials have been reported [24-26]. However, there are still few report about the synergistic anti-tumor treatment combined PTT with chemotherapy under NIR-laser-controlled drug release. Hence, with the aim to enhance superadditive or synergistic effects, we developed a DOX/IR-780-loaded temperature-sensitive-liposomes (DITSL) to combine PTT with chemotherapy and to achieve NIR-laser-controlled drug release for tumor treatment. In this system, IR-780 iodide, a lipophilic cation dye with peak absorption at 780 nm, was used as the PTT agents. The liposoluble IR-780 was incorporated into the lipid bilayer and soluble chemotherapeutic doxorubicin (DOX) in the hydrophilic core. The NIR-laser-controlled drug release of DITSL and their synergistic anti-tumor efficacy were investigated.

Materials and Methods

Materials

1,2-dipalmitoyl-sn-glycero-3-phosphocholine (DPPC), 1-myristoyl-2-palmitoyl-sn-glycero-3-phosphocholine (MPPC) and 1,2-distearoyl-sn-glycero-3-phosphoethanolamine-N-[methoxy(polyethylene glycol)-2000] (DSPE-PEG2000) were purchased from Avanti Polar Lipids Inc. (Alabaster, AL,USA). Doxorubicin and IR-780 were obtained from Sigma-Aldrich (St. Louis, MO, USA). The in situ Cell Death Detection Kit and DAPI were obtained from Roche (Mannheim, Germany). Cell Counting Kit-8 (CCK-8) was purchased from Dojindo Laboratories (Tokyo, Japan). Fetal bovine serum (FBS), Trypsin EDTA solution and Dulbecco's Modified Eagle's Medium (DMEM) were all purchased from Hyclone Laboratories (Logan, UT, USA). Female BALB/c mice, weighing about 20 g (6–8 weeks old), were obtained from Guangdong Medical Experimental Animal Center (Guangzhou, China). All other reagents were of analytical grade.

Preparation of DITSL

Liposomes (DPPC, MPPC and DSPE-PEG2000 in the molar ratio of 86: 10: 4) were prepared by the

established thin film hydration method [27]. Briefly, lipids and IR-780 were blended in chloroform (IR-780 : lipid = 5:100 in weight ratio), and the resultant solution was removed under nitrogen gas at room temperature. Any residual solvent of the lipid samples was subsequently removed under vacuum for a minimum of 3 h. The dried lipid films were hydrated at 65 °C with 250 mM $(NH_4)_2SO_4$ buffer (pH 5.4) and the suspension was extruded through a polycarbonate membrane of 200 nm using a mini-extruder (Avanti Polar Lipids, Alabaster, AL). Subsequently, the extra liposomal ammonium sulfate was replaced by PBS (137 mM NaCl, 2.7 mM KCl, 10 mM Na_2HPO_4, 2 mM KH_2PO_4, pH 7.4) overnight in a dialysis bag (MWCO 3500). DOX solution in PBS (1 mg/ml) was added to the liposomes and incubated at 65 °C for 4 h. DTSL, ITSL and empty liposomes were prepared by a similar approach in which DOX or IR-780 was added according to the requirement.

Characterization of DITSL

Size, surface charge and size distribution of all liposomes were determined using a dynamic light scattering detector Malvern Zetasizer (Nano ZS, Malvern, USA) at 25°C. The absorption spectra of DTSL, ITSL, and DITSL were obtained using Lambda25 UV/vis spectrometer (Perkin Elmer, USA) with excitation at 480 nm to monitor DOX and at 780 nm to monitor IR-780. The encapsulation efficiency (EE) of DOX or IR-780 was determined as follows: isolating the fresh liposomes from aqueous suspension medium by ultracentrifuge (20,000 r/min, 30 min) (Optima MAX-XP, Beckman, USA). The supernatant containing the free drugs was removed. Then the concentrations of IR-780 and DOX were determined by fluorescence spectrometry (F900, Edinburgh Industries, UK). The EE is calculated according to the following formula: EE (%) = (weight of loaded drug)/ (weight of initially added drug) ×100.

Stability test of DITSL in biological buffers

The long-term stability of the TSL formulations was tested by incubating samples of DITSL suspension (1 mM lipid) in buffer (20 mM HEPES with 5% glucose, pH 7.4) and buffer containing 30%, 50%, or 90% fetal bovine serum (FBS). Incubation was kept at 37 °C for 24. Samples without incubation were considered as a blank control (I_0). Samples mixed with TritonX-100 as positive controls (I_{100}). The released DOX in the supernatant was determined by fluorescence spectroscopy with emission at 593 nm and excitation at 480 nm. The percentage of DOX release was calculated as $(I_t - I_0)/ (I_{100} - I_0) \times 100$.

NIR laser-induced temperature increase in vitro

0.5 mL of PBS, DTSL (DOX: 15 μg/mL), ITSL (IR-780: 15 μg/mL) and DITSL (IR-780: 15 μg/mL, DOX: 15 μg/mL) were added into the well of 24-well plate. NIR laser (808 nm, 0.8 W/cm^2) was used to irradiate the samples for 5 min. The changes of temperature were obtained by infrared imaging camera (Ti27, Fluke, USA).

Temperature-dependent and laser-triggered drug release

Temperature-dependent release profile of DOX from DITSL was detected by fluorometry by incubating these DITSL samples in a thermostatically controlled dry bath (Labnet International, Rutland, UK). When the temperature of the solution reached 37 °C, 42 °C or 50 °C, it was maintained at the desired temperatures for 0.33, 0.67, 1, 2, 3, 4, 5, 10 or 30 min. The laser-triggered release experiments were performed with 0.8 W/cm^2 808 nm laser irradiation (Leimai, China) for 5 min using DTSL or DITSL respectively. DITSL which received laser irradiation was also used as a control. To realize the switch on/off behavior, DITSL solution was irradiated with 808 nm laser (0.8 W/cm^2) for 2-min each hour. Experiments were repeated three times. The DOX release (%) was calculated as stated above.

In vitro cellular uptake

The cellular uptake of DTSL, ITSL and DITSL in 4T1cells was examined using confocal microscopy. Briefly, 4T1 cells (2 × 10^4 cells/well) were seeded into 6-well chambered cover glasses (Lab-Tek, Nunc, USA) in 200 μL medium. After 24 h, the medium was replaced with the medium containing DTSL (10 μg/mL DOX), ITSL (10 μg/mL IR-780) or DITSL (10 μg/mL DOX and 10 μg/mL IR-780). After 3 h incubation, the cells were washed thrice with PBS and fixed with 4% paraformaldehyde solution for 20 min. After stained with DAPI. These cells were observed by confocal laser scanning microscope (CLSM) (Leica TCS SP5, Germany).

Cellular drug release of DITSL

4T1 cells (2 × 10^4 cells/well) were seeded into 8-well chambered cover glasses in 200 μL medium. After overnight cultivation at 37 °C, medium was replaced by fresh medium containing DITSL (10 μg/mL DOX and 10 μg/mL IR-780). After 1 h incubation, the cells were washed for thrice and stained by DAPI. After that, 4T1 cells were treated with laser irradiation (808 nm, 0.8 W/cm^2, 5 min) or incubated at 37 °C or 42 °C for 5 min, respectively. The cellular DOX fluorescence signals pre- or

post-treatment were then observed by CLSM and the fluorescence signal intensities were quantified.

In vitro photothermal, chemo-photothermal efficiency

4T1 cells were seeded in 96-well plates (4×10^3 cells/well) for overnight. Empty liposomes, DTSL, ITSL or DITSL were added to the media at 10 μg/mL final DOX or IR-780 concentrations. The DITSL group kept the equivalent IR-780 dosage with ITSL group and an equal content of DOX with DTSL group. After 3 h incubation at 37 °C, the cells were rinsed twice and replaced with fresh culture medium. Then these cells treated without or with laser irradiation at 0.6 W/cm^{2}or 0.8 W/cm^2 for 5 min. After 24 h incubation, cell viability was determined by the Cell Counting Kit-8 kit (Dojindo, Japan) by measuring the absorbance at 450 nm using a multimode plate reader (Synergy™ 4, BioTek, VT, USA). To visually observe the photothermal or chemo-photothermal therapeutic efficacy, the 4T1 cells were seeded onto 24-well plate (7×10^4 cells/well) and incubated for 24 h. The cells were irradiated with or without a 0.8 W/cm^2 808 nm laser for 5 min as stated above. After another 24 h incubation, cells were washed with PBS and then stained with Calcein-AM/PI double staining Kit, followed by observation under microscope.

Animal models

All animal experimental protocols were reviewed and approved by Shenzhen Institutes of Advanced Technology, Chinese Academy of Sciences Animal Care and Use Committee. The methods were carried out in accordance with the approved guidelines. 4T1 cells were harvested and suspended in PBS at a density of 2×10^6 cells/mL. 100 μL of the tumor cell suspension was injected into the right flank of female BALB/c mice. Tumor treatment was initiated when the tumor volume reach 100-200 mm^3. Tumor sizes were measured every 3 days. Tumor volume (mm^3) = (length×width^2)/2.

In vivo temperature measurements during NIR irradiation and chemo-photothermal therapy

The mice bearing 4T1 tumors were intratumorally injected with 100 μL of ITSL or DITSL to determine the intratumoral temperature changes during NIR laser irradiation. Mice bearing the 4T1 tumor were also injected with 100 μL of PBS as a control. The tumors were irradiated by the 808 nm laser at 1 W/cm^2 for 5 min. Region maximum temperatures and infrared thermographic maps were obtained with the infrared thermal imaging camera. Treatments were started when the tumors reached a volume of 100-200 mm^3. The mice were divided into seven groups that were treated with PBS, DTSL, ITSL and DITSL with or without NIR irradiation, respectively. All agents were intratumorally injected at doses equivalent to 20 μg of IR-780 or 20 μg of DOX. For the laser treatment groups, the tumors were exposed to the NIR laser at 1 W/cm^2 for 5 min. The tumor size of each mouse were recorded. Mice with tumor sizes exceeding 1000 mm^3 were euthanatized according to the animal protocol.

H&E staining and immunofluorescence staining

The mice were sacrificed by standard decapitation, and the tumors were harvested, fixed with formalin and embedded in paraffin. 7-μm sections were cut with a paraffin slicing machine, followed by staining with hematoxylin-eosin (H&E) dyes. Tumor apoptosis was also assessed by TUNEL assay according to the product instruction. Slides were stained with rat anti-mouse CD31 antibody (eBioscience, San Diego, CA) to assess tumor blood vessels.

In vivo contrast-enhanced ultrasonography

To assess tumor blood vessels in the early stages of photothermal-/chemo-therapy, mice were treated with PBS, DTSL, ITSL and DITSL with or without NIR irradiation as stated above. After 24 h, the combined therapy effect was evaluated by ultrasound (US) imaging. Briefly, the mice from all groups were intravenously injected with 1×10^8 microbubbles to further analyze the tumor blood perfusion. The increasing US contrast signals were observed in vivo under US contrast-mode. All images were acquired using a high-frequency Philip IU22 probe (frequency: 9 MHz, and a mechanical index: 0.07).

Statistical analysis

All values shown are in mean ± SD unless otherwise indicated. ANOVA was used for statistical analysis by SPSS software. The differences were considered to be significant for * $P < 0.05$, and to be very significant for ** $P < 0.01$.

Results and discussion

Preparation and characterization of DITSL

Figure 1A presented the preparation process of DITSL. Briefly, the DITSL were first self-assembled from IR-780, DPPC, MPPC, and DSPE-PEG2000 through a thin-film rehydration method. The soluble DOX was then encapsulated into the liposomes by the ammonium sulfate gradient method. Obviously, the resulting DITSL appeared dark brown, demonstrating both IR780 (green) and DOX (red) were encapsulated into the nanoparticles (Fig.1B, inset). Due to the

difference of solubility, the hydrophobic IR-780 would be encapsulated into the lipid bilayer of DITSL and the hydrophilic DOX would exist in the core of TSL. The presence of IR-780 in the lipid bilayer makes it easy to destruct the shells after receiving laser irradiation and gives a greater chance for encapsulated drugs to escape from nanocarriers and to avoid thermal inactivation. The size, surface charge and encapsulation efficiency of particles were summarized in Table 1. The average particle size of DITSL was approximately 138.98 ± 8.74 nm, with a polydispersity index (PDI) of 0.32 ± 0.02. By contrary, ITSL, DTSL and empty liposomes had smaller particle size, with 94.05 ± 1.74 nm, 84.55 ± 7.41 nm and 77.53 ± 4.44, respectively (Fig.1B and Table 1). The zeta potential of these particles appeared negative, with -11.54 ± 0.52, -10.74 ± 0.41, -9.57 ± 0.12 or -8.21 ± 0.24 for DITSL, DTSL, ITSL or empty liposomes, respectively. The encapsulation efficiencies of IR-780 and DOX in DITSL were 94.47% and 92.52%. For DTSL and ITSL, the IR-780 or DOX encapsulation efficiency was slightly high than that of DITSL, achieving 99.98% for IR780 and 97.39% for DOX, which was similar to the previous reports [28-30].

The absorption spectra showed the ITSL had strong absorption peak at 793 nm. The absorption peak of DTSL was at 492 nm, in agreement with the absorption characteristic of free DOX. As expected, the absorption curve of DITSL appeared two obvious peaks. The one was located at 793 nm which belongs to the characteristic absorption of IR-780 and another at 492 nm which belongs to the absorption of DOX (Fig.1C). Such a strong absorption of DITSL in NIR region indicated a potential for PTT upon laser irradiation. In fact, evidences have demonstrated that IR-780 can act as an excellent PTT agent [28, 31].

In order to evaluate the stability of these DITSL in different biologically relevant media, DOX leakage was measured over time in PBS, 30% serum, 50% serum or 90% serum at 37 °C. DITSL in 90% serum released 100% of encapsulated DOX after incubation for 24 h. (Fig. 1D, red line). Under 50% and 30% serum conditions, DITSL showed a higher stability, releasing 57% (Fig. 1D, orange line) and 53% (Fig. 1D, green line) DOX after 24 h, respectively. It was notable that DITSL appeared stable and minimal drug release in PBS (about 23% after 24 h incubation) was observed (Fig. 1D, black line). These results suggest TSL had good stability in PBS, but not in high concentration serum conditions. Similar results were also published by other groups [32, 33]. The instability in the high serum condition may ascribe to the presence of lysolipid in the lipid bilayer that can exchange and translocate with various blood components, leading to a series of events, such as thinning liposome membrane, pore-forming defects and drug leakage following burst-release kinetics [27, 34].

Table 1. Characterization of liposomes.

Liposomes	D/L ratios	Diameter (nm)	Zeta potential (mV)	PDI	EE (%)
Empty lipo	-	77.53 ± 4.44	-8.21 ± 0.24	0.23 ± 0.05	-
ITSL	1:20	94.05 ± 1.74	-9.57 ± 0.12	0.28 ± 0.03	99.98%
DTSL	1:20	84.55 ± 7.41	-10.74 ± 0.41	0.24 ± 0.03	97.39%
DITSL	1:20	138.98± 8.74	-11.54 ± 0.52	0.32 ± 0.02	92.52% (DOX) 94.47%(IR-780)

Note: D: drug; L: liposome; EE, encapsulation efficiencies.

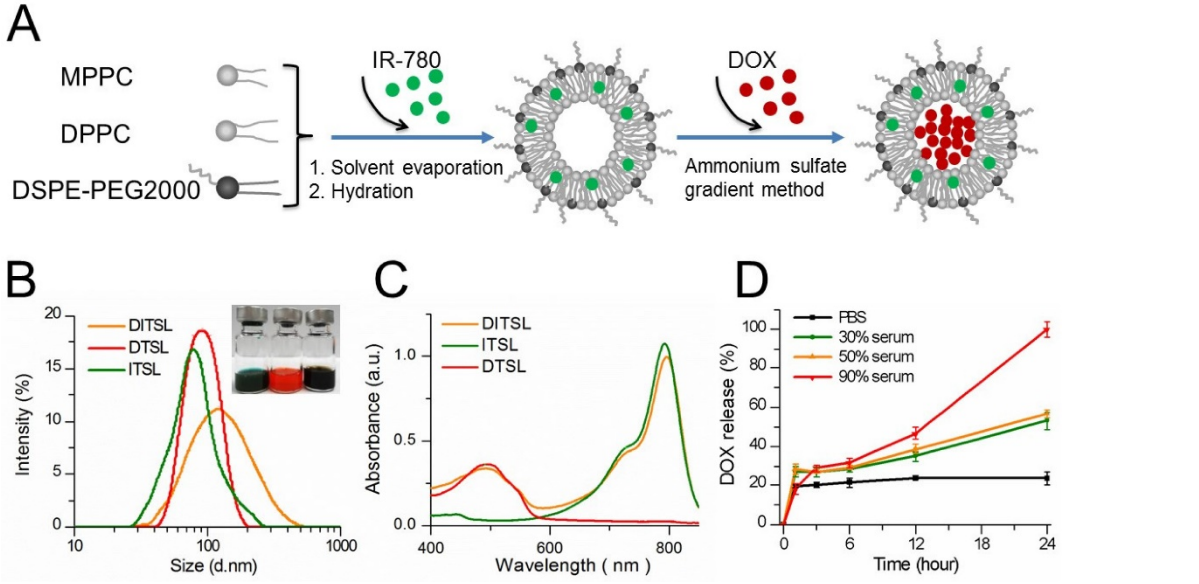

Figure 1. Synthesis and characterization of DITSL. (A) Schematic diagram of preparation of DITSL. (B) The size distribution of DITSL by dynamic light scattering. Inset shows a photograph of ITSL (green), DTSL (red), DITSL (brown) solution. (C) UV-vis absorbance spectra of the dispersions containing DTSL (red), ITSL (green) or DITSL (brown). (D) The short-term drug release effects of DITSL incubated at 37 °C in PBS buffer (pH 7.4) or in the presence of 30%, 50% or 90% fetal calf serum. Data points are an average of three replicates.

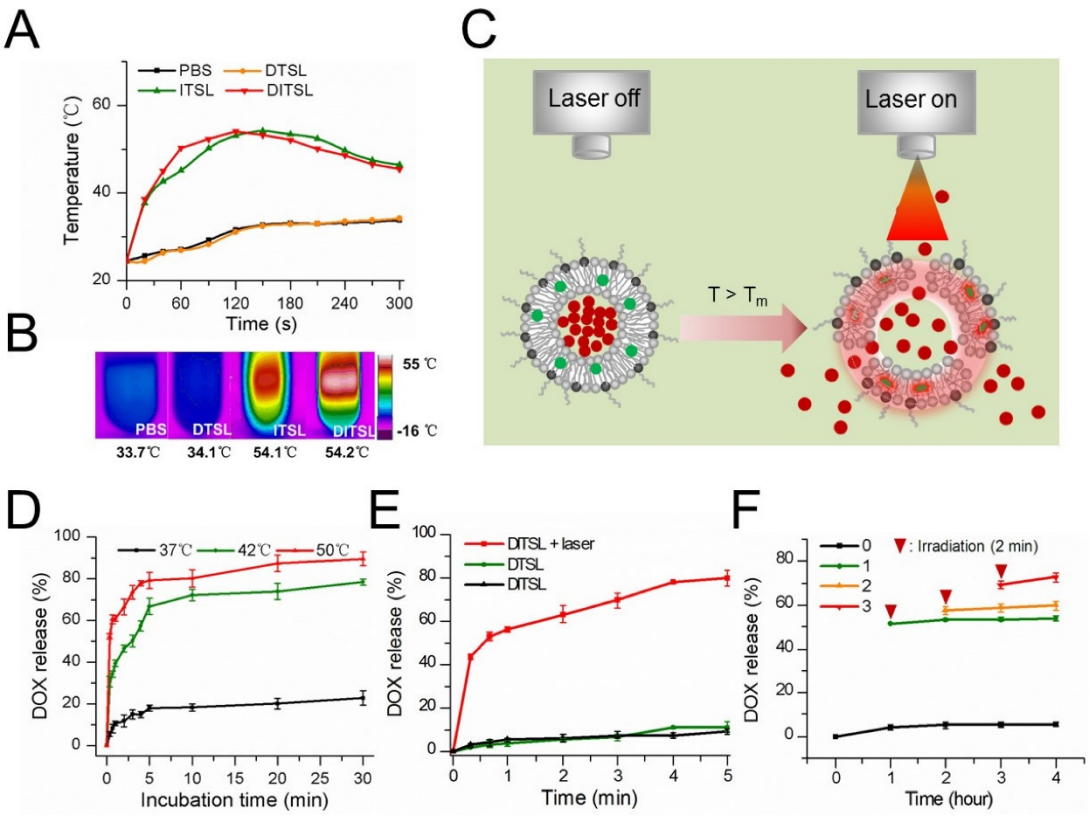

Figure 2. The photothermal effects of DTSL, ITSL or DITSL and heating-induced DOX release from DITSL. (A) The temperature profiles of PBS, DTSL, ITSL and DITSL dispersions under the irradiation of 808 nm laser. (B) The peak temperature maps were recorded with an infrared thermal imaging camera. (C) Schematic diagram of DOX release from DITSL under NIR-laser irradiation. The liposome membrane temperature would increase when the NIR-laser irradiation was applied. Destruction of liposome membrane occurs when the liposome membrane temperature achieves 42 °C. (D) The cumulative release of DOX from DITSL at 37 °C, 42 °C or 50 °C. (E)The cumulative release of DOX from DTSL or DITSL under the NIR-laser irradiation at a power intensity of 0.8 W/cm² for different time (0-5min). The cumulative release of DOX from DITSL without irradiation was also examined as a control. (F) The effects of irradiation-nonirradiation sequence number of 0 time, 1 time, 2 times or 3 times on the released DOX from DITSL with 808 nm laser (0.8 W/cm², 2-min). Data represents the mean ± standard deviation of triplicate measurements.

Drug release properties of DITSL

To evaluate the photothermal efficiency of DITSL, we monitored the temperature changes under laser irradiation in vitro using an infrared thermal imaging camera. With the laser irradiation at 0.8 W/cm² for 5 min, the temperature of DITSL and ITSL maximally increased to 54.2 °C and 54.1 °C, while the PBS and DTSL only increased to 9.3°C and 9.7 °C and finally reached about 34 °C (Fig. 2A-2B). The results showed IR-780 but not DOX produced significant temperature elevation under laser irradiation, giving them the PTT potentials to producing irreversible damage to tumor cells [35, 36]. Furthermore, high temperature above the phase transition temperature (>42°C) might destruct lipid bilayer of liposomes, which would result in a fast and laser irradiation-controlled DOX release from DITSL (Fig. 2C).

To test the temperature-sensitive drug release capability, DITSL samples were heated in a thermostatically controlled dry bath. DITSL displayed a clear temperature-dependent DOX release profile upon exposure to hyperthermia (42 °C or 50 °C) but not to body temperature (37 °C) (Fig. 2D). DITSL released up to 40% and 61% of their contents in the first minute at 42 °C and 50 °C, respectively. By contrast, similar conditions, but now at a temperature of 37 °C, hardly caused content release from DITSL (< 20%). When the temperature remained at 42 °C, the release rate increased from 47.6% ± 4.2% to 64.4% ± 6.2% as the incubation time increased from 10 min to 20 min. DOX release achieved approximately 78% and 90% in 30 min at 42 °C and 50 °C, respectively. The results indicate that the release efficiency of DOX increased with the increment of temperature and duration of incubation, indicating that the TSL is sensitive to the temperature changes.

Next, the efficiency of NIR-laser-induced drug release was examined and the results were shown in Fig. 2E. Obviously, the rate of drug release from DITSL increases as the laser irradiation time. In contrast, DTSL without IR-780 did not show NIR-laser-induced drug release. The cumulative release of DOX from DTSL was 1.9 % at the first 20 seconds when DITSL released almost 43.5 % of its contents. After 5 min of laser irradiation, the efficiency of drug release attained 80.1% ± 3.9% for DITSL,

which was much higher than that of DTSL received the same laser irradiation or of DITSL not received laser irradiation. The NIR-laser controlled DOX release might attribute to IR-780 in DITSL which can convert laser energy into heat, leading to the temperature increase (>42 °C) and then triggering drug release (Fig. 2C). Fig.2F demonstrated DITSL had good controllability under laser irradiation. Without laser irradiation, the cumulative release of DOX from DITSL solution was only 4.2% at room temperature (RT) after 1 h and nearly retained the same within the later 4 h (Fig.2F, black line). After the first 2-min irradiation (T>42 °C) at 1 h, the cumulative release of DOX (Fig.2F, green line) increased remarkably and jumped to 50.6%, and almost remained unchanged during the subsequent non-irradiation periods (RT for 3 h), indicating 2-min on/long-time off releasing behavior. Similarly, after the second 2-min irradiation (T>42 °C) at 2 h, an obvious increasing cumulative release of DOX was acquired (Fig.2F, orange line) and climbed to 59.5%. It also kept nearly no increasing in the non-irradiation term (RT for 2 h). At last, the third 2-min irradiation (T>42 °C) at 3 h led to a slight rise for the released DOX to 70.9%, which also stayed same in one hour later (RT). This NIR-laser-switched release process was attributed to the controllable temperature cycle (above or below 42 °C) of DITSL solution, which is different from the traditional endogenous [37,38] or exogenous [39-42] stimuli-responsive nanocarriers that usually are spontaneous and/or cannot be shut down. Based on the above the DOX release results, DITSL can present a completely controlled drug release platform through regulating the frequency and power of laser irradiation.

In vitro cellular uptake and drug release

Murine breast cancer 4T1 cells were treated with ITSL, DTSL and DITSL to evaluate the cellular uptake of those particles. When a cross section of liposomes-treated cells was observed by confocal laser scanning microscope, DOX mainly localized in the cell nucleus in 4T1 cells, while IR-780 was homogenously distributed in the cytoplasm in 4T1 cells (Fig.3). This results showed ITSL, DTSL and DITSL could be easily uptaken by 4T1 cells. Interestingly, DITSL-encapsulated DOX could be detected both in the cytosol and the nucleus of 4T1 cells. The possible reason could be that DOX molecules released from the liposomes entered into the cell nucleus, while DOX entrapped in liposomes was still in the cytosol because of size limitation, preventing them entering into the cell nucleus [11, 43-45].

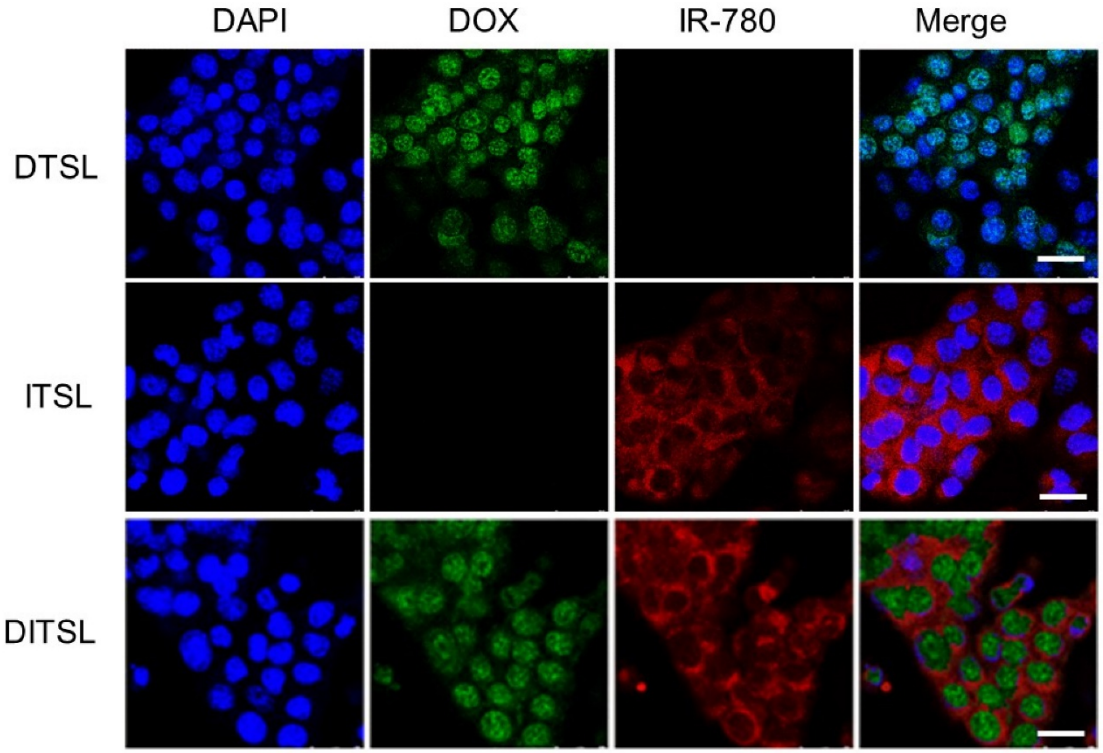

Figure 3. The in vitro cellular uptake. (A) Confocal fluorescence images displayed cellular localization of DOX and IR-780 after 3 h incubation with DTSL, ITSL or DITSL. Blue represented the fluorescence of DAPI, green represented the fluorescence of DOX and red represented the fluorescence of IR-780 (Scale bar, 25 μm).

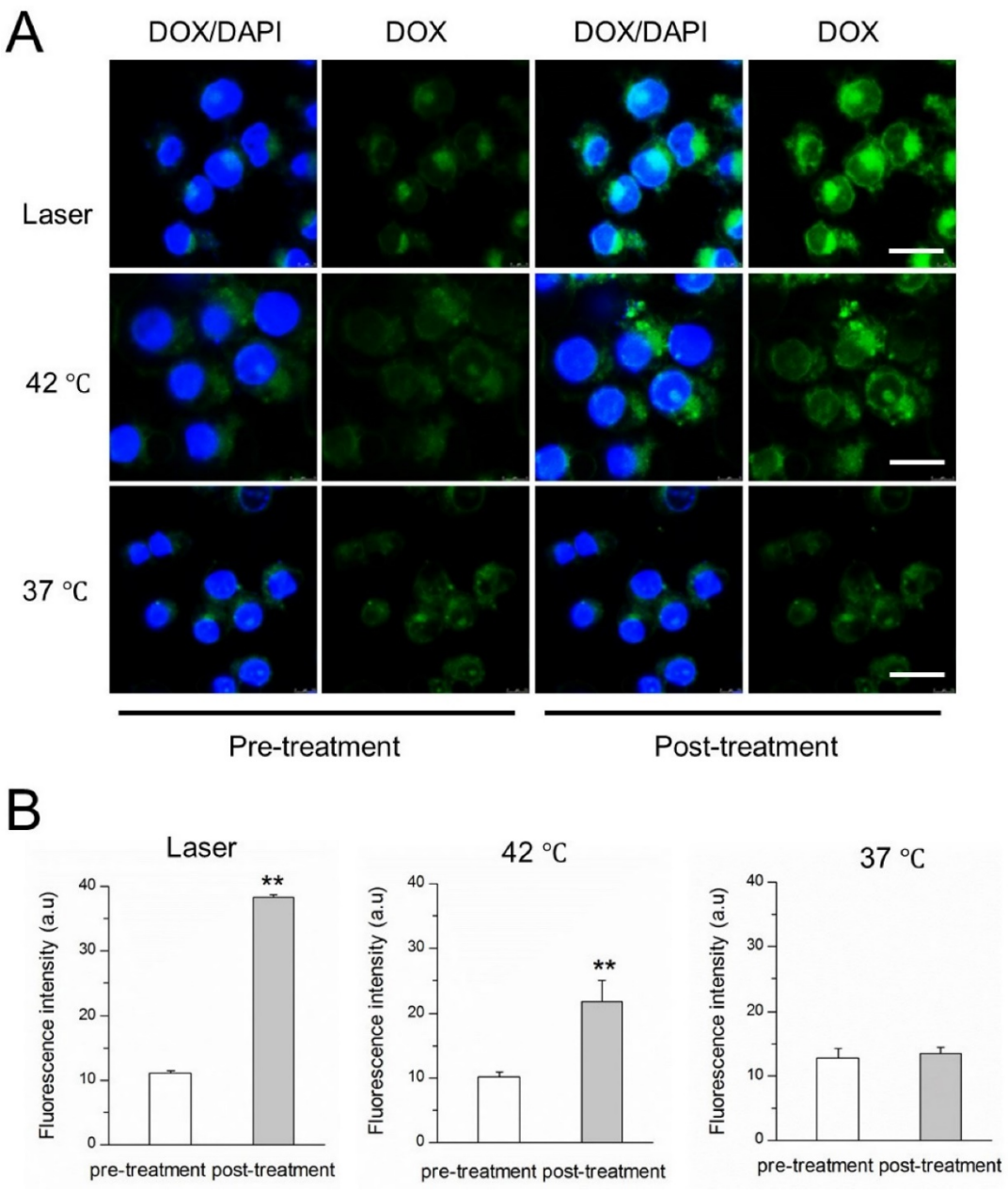

Figure 4. NIR laser-induced drug release from DITSL in 4T1 cells. (A) CLSM images of 4T1 cells which contained DITSL before and after laser irradiation treatment or incubation with 42 °C or 37 °C pre-warmed PBS for 5 min. Nuclei were stained with DAPI (blue), and green was the fluorescence of DOX. (B) Quantitative analysis of fluorescence intensities of DOX before and after treatments. Scale bar = 20 μm.

The NIR-laser-controlled drug release was then studied at a cellular level using confocal laser scanning microscope. 4T1 cells were incubated with DITSL and then replaced with pre-heated PBS or irradiated by laser. The images were shown in Fig.4A, showing the significantly stronger DOX fluorescence signals from the cells after irradiated by laser for 5 min, compared with the fluorescence intensity of the cells which did not receive laser irradiation. A similar DOX fluorescence enhancement was also found in these cells treated with 42 °C pre-heated PBS. The quantitative analysis revealed there were 3.45- or 2.14-fold higher DOX fluorescence intensities after these cells received with laser irradiation (Fig.4B, left) or 42 °C pre-heated PBS treatment (Fig.4B, middle). In contrast, there was not significantly enhanced DOX fluorescence signals for these cells which were kept at 37 °C, indicating minimal DOX release at 37 °C (Fig.4B, right). Our results demonstrated that the laser- or water bath-caused hyperthermia could disrupt DITSL, leading to rapid drug release from liposomes.

In vitro chemothermal, photothermal and chemo-photothermal treatments

To evaluate the in vitro cytotoxicity of the

chemotherapy, photothermal therapy, and chemo-photothermal therapy, the viability of cells was determined by CCK8 assay. 4T1 cells were incubated with PBS, DTSL, ITSL or DITSL for 4 h, followed by receiving with or without laser irradiation. Fig. 5A showed that liposome carriers had not cytotoxicity to the tumor cells when compared with PBS control (P>0.05). Chemotherapy with DTSL containing 10 μg/mL DOX showed an obvious cytotoxicity, with 59.4% cell viability when these cells received or did not received with laser irradiation. PPT with ITSL under a 0.6 W/cm^2 power density laser (10 μg/mL of IR-780 dose) showed significant cytotoxicity with 43.6% cell viability, much lower than that of the cells incubated with the same ITSL dose without laser irradiation. Notably, the treatment with DITSL and laser irradiation induced the strongest cytotoxicity, with significantly lower viability than that of the cells received with DL, ITSL + laser irradiation or DITSL without laser irradiation. There had a similar change trend when using a higher laser irradiation power (0.8 W/cm^2), showing a stronger cytotoxicity in these PTT treatment groups. The cell viabilities were 17.8% and 9.5% when those cells treated with DITSL containing 10 μg/mL IR-780 were exposed to 0.6 and 0.8 W/cm^2 laser irradiation, respectively (Fig.5B).

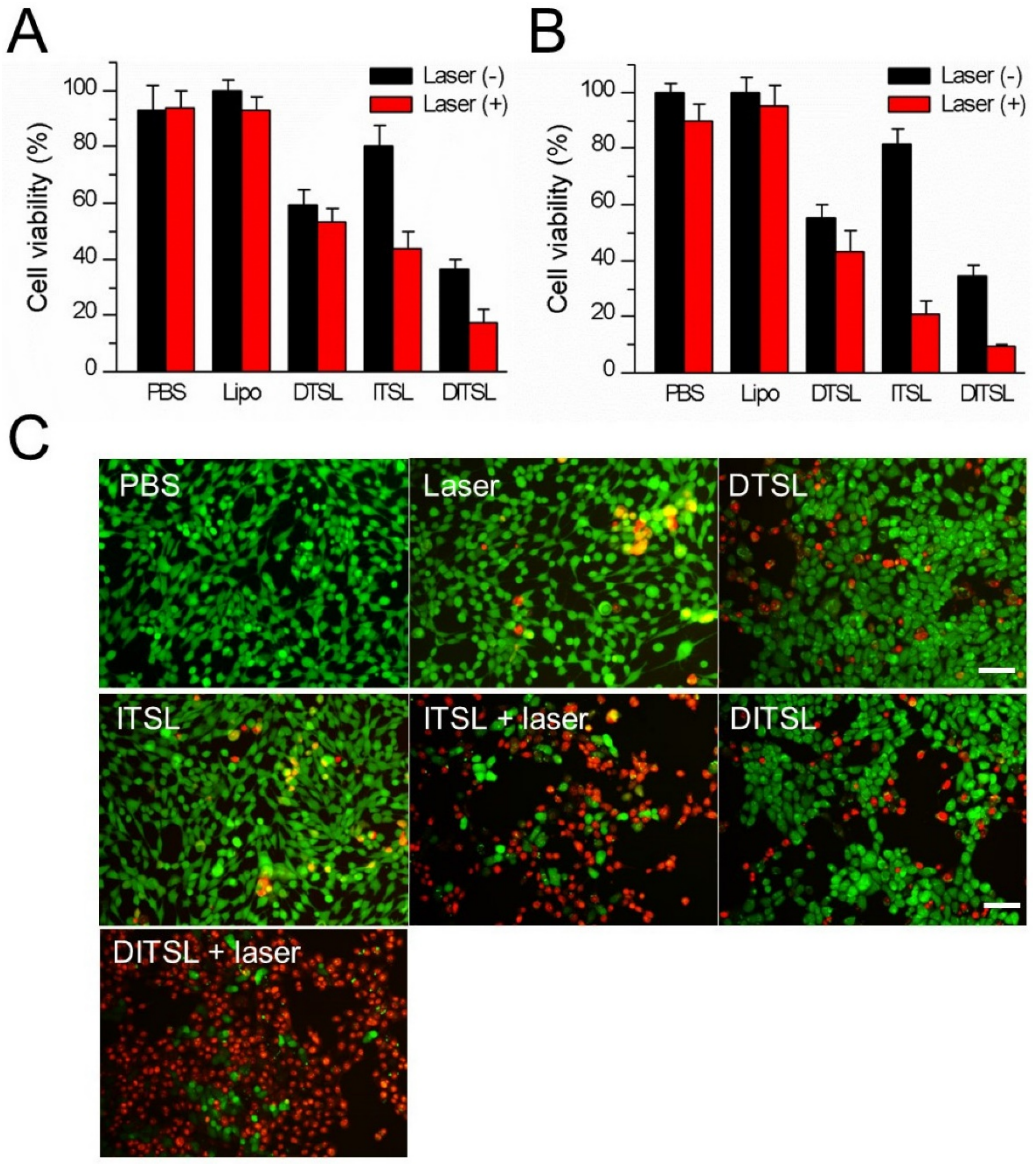

Figure 5. Cell viability after chemo-photothermal treatment. (A) Quantitative evaluation of cell survivals incubated with PBS, empty liposomes, DTSL, ITSL and DITSL with or without laser irradiation (0.6 W/cm^2, 5 min), showing much lower cell viability in the cells receiving DITSL plus laser irradiation. (B) Increasing the laser intensity (0.8 W/cm^2, 5 min) resulted in significantly lower cell viability in these cells incubated with ITSL or DITSL. (C) Fluorescence images of 4T1 cells after chemo-photothermal treatment. Viable cells were stained green with calcein-AM, and dead/later apoptosis cells were stained red with PI. Scale bar = 25 μm. The data was shown as mean ± SD; (*) P < 0.05, (**) P < 0.01.

Compared with DITSL + laser irradiation, the relatively lower cell-killing ability of DTSL and ITSL could be attributed to delayed DOX release from DTSL or insufficient ITSL to produce enough heat to kill cells under laser irradiation. The mechanism of the synergistic effect is supposed to be an enhanced cytotoxicity of DOX in elevated temperature and increasing heat sensitivity of cells exposed to DOX [6, 17]. To further observe the efficacy of the combination of PTT with chemotherapy, the treated cells were stained with Calcein-AM and PI to identify live and dead/late apoptotic cells, respectively. Fig.5C showed that there were just a few dead cells (red) in the group received with laser irradiation alone, suggesting the relatively safe laser irradiation at 0.8 W/cm² power density. With or without laser irradiation, DTSL induced similar ratios of dead cells. As expected, ITSL with laser irradiation induced lots of dead cells. Before laser irradiation, the DITSL-treated cells had the same survival as the DTSL-treated cells. Once laser irradiation was excited to the DITSL-containing cells, a large number of cells were killed by thermal energy and cytotoxicity of DOX. The results suggested that the cytotoxic effect of DITSL on 4T1 cells could be boosted by the laser irradiation.

In vivo NIR imaging and the anti-tumor efficiency

The NIR fluorescence imaging data showed a relatively slower fluorescence decrease of DITSL than free IR-780 in physiological environments after 5 days, indicating the increased accumulation of DITSL in the tumor (Fig. S1). Since the temperature increase plays a key role to induce cell death in PTT, we next examined intratumoral temperature profiles during PTT. Tumors treated with ITSL or DITSL followed by laser irradiation for 5 min showed a significant and fast temperature elevation in the localized tumor regions, achieving the peak temperatures of 61.0°C for ITSL or 61.3 °C for DITSL after 2 min. In contrast, the PBS-treated tumor for the same NIR irradiation showed a slight temperature elevation (Fig. 6A-6B).

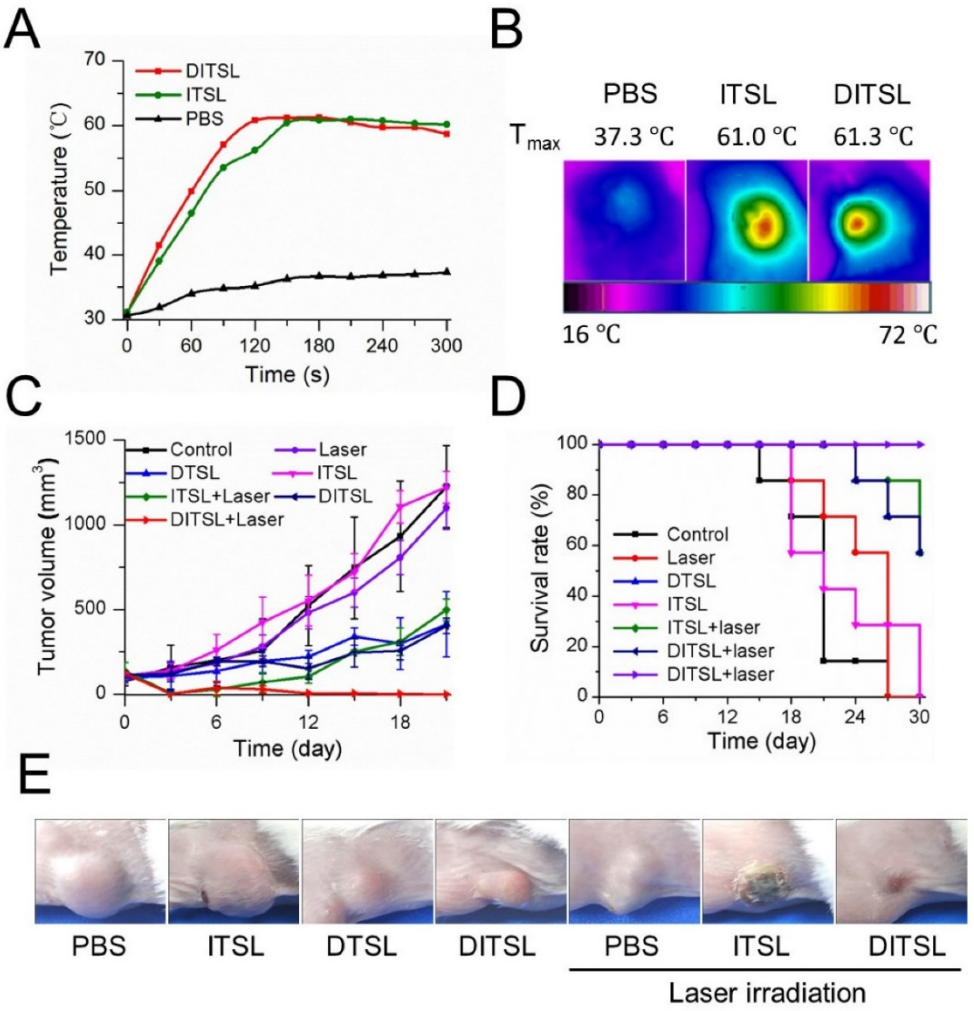

Figure 6. The anti-tumor efficacy in vivo. (A) The temperature change profiles of the irradiated tumors received with PBS, ITSL or DITSL from 0-5 min. (B) The representative infrared photothermal images of the tumors after laser irradiation. (C) The tumor growth curves of mice receiving PBS, only laser irradiation, DTSL, ITSL, DITSL without laser irradiation, ITSL+ laser or DITSL+ laser. Combined treatment of DITSL+ laser produced better synergistic anti-tumor effect and no tumor recurrence was noted. (D) Survival curve of the tumor-bearing mice after different treatments. (E) Representative images of these tumors after treatments.

Although the focus temperature of laser irradiation may exceed the damage threshold (>50°C) and be enough to induce irreversible tissue damage, it is still notable that the temperature of larger surrounding regions of tumors might be sublethal. It was reported that hyperthermia-induced cell death has different mechanisms according to the different temperatures. The tumor temperature above 50°C might induce irreversible cell injury, while the tumor temperature between 41°C and 45°C might induce the sublethal effects, such as expression of apoptosis genes, caspases activation and mitochondrial damage [1]. These sublethal and reversible cell responses may result in incomplete ablation and tumor recurrence [46, 47]. If drugs could be released from DITSL which was localized at the sublethal tumor regions, it would greatly inhibit the reversible cell responses and accelerate their death. To demonstrate how the dye/drugs are getting redistributed post release induced by laser irradiation, we examined the fluorescence areas of IR-780 before and after laser irradiation. The result was presented in Fig. S2. When laser irradiation was not used, the distribution area of the dye was not increased after 6 h. In contrast, upon these tumors received laser irradiation, the distribution area of the dye significantly increased after 6 h and became larger after 24 h. It indicates the release of the dye was promoted after the DITSL was exposed to laser irradiation. In order to determine the combined therapeutic efficacy of photothermal-/chemo-therapy, the tumor-bearing mice received PBS, ITSL, DTSL or DITSL with or without irradiation. The tumor growth curves were presented in Fig. 6C. Obviously, control tumors treated with PBS, only NIR irradiation, or ITSL without laser irradiation grew rapidly. No statistically significant differences were found in final tumor sizes ($P > 0.05$). This indicated that tumor growth was not affected by either ITSL or NIR irradiation alone. For ITSL + laser group, the growth of tumors suffered a significant inhibition after 3 days (v.s. PBS or ITSL without laser irradiation, $P<0.01$), but boosted rapidly in the subsequent term (from 12 to 18 days), eventually reaching about 3.6-fold tumor volume compared to that at first day. This fact demonstrated that the growth of tumor could be partly inhibited by photothermal effects from ITSL. The growth of 4T1 tumors was slightly inhibited by DTSL or DITSL without NIR laser irradiation. There was no significant difference between two groups, indicating that DITSL without laser irradiation mainly play a chemo-therapy role (similar with DTSL) (Fig.6C). DOX is a well-known chemotherapeutic agent to a breast tumor. Usually, it requires multiple and high dosages to achieve a satisfying anticancer effect. In this study, mice were treated with only a single dose of DOX, which was not sufficient to suppress tumor growth in vivo. Quite discrepantly with other groups, the volume of tumors from DITSL + laser group showed continuous decrease and led to a complete remission (all $P<0.05$), leaving the original tumor site with scars which fell off about 1 weeks later (Figure 6E). Kaplan–Meier survival analysis with log-rank test was conducted to assess the survival time of these mice and the results are summarized in Fig.6D. The DITSL + laser group exhibited the longest median survival time (MST) in comparison to the PBS group and the other treatment regimens. Of note, 100% of the animals treated with the chemo-photothermal combination survived until the end of the study period of 30 days. No tumor recurrence was observed in this group. During the animal experiments, the body weight of these tumor-bearing mice showed no significant changes in all groups (Fig. S3). The toxicologic assessment of DITSL by hemolytic test and histopathologic examination did not observe hemolysis and significant damage to the mouse main organs (Fig. S4 and S5).

To further confirm the antitumor effects of DITSL mediated chemo-photothermal therapy, histological analysis for these tumors were performed by using of H&E staining and TUNEL staining. Significant tumor necrosis with severe structural damage and more apoptotic cells (strained brown) could be observed in the tumors receiving DITSL and laser irradiation (Fig.7). DTSL or ITSL plus laser irradiation showed moderate apoptotic cells. In comparison, tumors receiving PBS, only laser, ITSL without laser irradiation showed no or little apoptotic cells, further demonstrating the combined therapeutic efficacy of photothermal-/chemo-therapy mediated by DITSL and laser irradiation.

In fact, some studies for chemo-photothermal therapy with different chemo-drugs and heat-generation materials have been reported. Zheng M, et al reported DOX/ICG loaded lipid-polymer nanoparticles for chemo-photothermal combination therapy [11]. Needham D, et al demonstrated the importance of rapid hyperthermia-triggered liposomal drug release from the thermosensitive liposome at the tumor site and may account for the enhanced therapeutic effect [24]. Zhang H, et al reported thermosensitive liposome formulated indocyanine green (ICG) for near-infrared triggered photodynamic therapy for triple-negative breast cancer [25]. Guo F, et al used IR780 as the heat-generation materials to design a dual-functional thermosensitive bubble-generating liposome (IR780-BTSL-FA) to realize enhanced therapeutic and diagnostic functions [26]. Although these reports are

similar with our study, there are many difference between them. Firstly, most of them used ICG as heat-generation agents, while we utilized IR-780 in our study. Secondly, the compositions consisted of temperature-sensitive liposomes are different. The previous reports used PLGA or DPPC as the main compositions in their study while we used MPPC and DPPC as the main compositions of temperature-sensitive liposomes. According to Needham D' reports [24, 48], the incorporation of MPPC into the gel phase liposomes composed of DPPC can achieve a significantly enhanced release of entrapped liposome contents at mild hyperthermic temperatures in a matter of seconds in comparison with the more conventional (DPPC/DSPC-based) temperature-sensitive liposomes. Although IR-780 was used as the heat-generation materials in Guo F's report, only 75.4% DOX was released from their carriers 8 h after laser irradiation. In contrast, the total release of DOX from our DITSL was 43.5 % at the first 20 seconds and achieved 80.1% after 5 min of laser irradiation. Noteworthy, a lower laser irradiation power (0.8 W/cm^2) was used in our study. Obviously, our laser-triggered drug release system was faster and more effective than that of their constructs. Moreover, we found that there was a higher drug encapsulation efficiency (92.52% for DOX) in our system compared with their carriers. Thus, the higher drug encapsulation efficiency and more effective drug release efficiency from our system resulted in a relatively higher anti-tumor efficacy in vitro and in vivo.

In vivo tumor blood vessels detection

Contrast-enhanced-ultrasound (CEUS) and immunofluorescence staining were also used to assess tumor blood vessels in the early stages of photothermal-/chemo-therapy. Tumors were injected with PBS, DTSL, ITSL or DITSL with or without NIR laser irradiation, followed by ultrasonographic examinations under contrast-mode after 48 h. Fig.8A and Fig.8B demonstrated that there had significantly enhanced US signals in the tumors treated with PBS, DTSL, ITSL or DITSL without laser irradiation, indicating abundant blood vessels in these tumors. By contrast, lower CEUS signals or defective tumor areas were observed in the tumors treated with ITSL or DITSL after laser irradiation. Notably, there had larger defective areas in the DITSL + laser-treated tumors in comparison with ITSL + laser-treated tumors ($P<0.01$), showing the drugs released from DITSL might take part role in inhibiting tumor angiogenesis or tumor growth. Immunofluorescence staining results revealed CD31-positive cells (CD31 is a marker for vascular endothelial cells) was significantly decreased after combination therapy

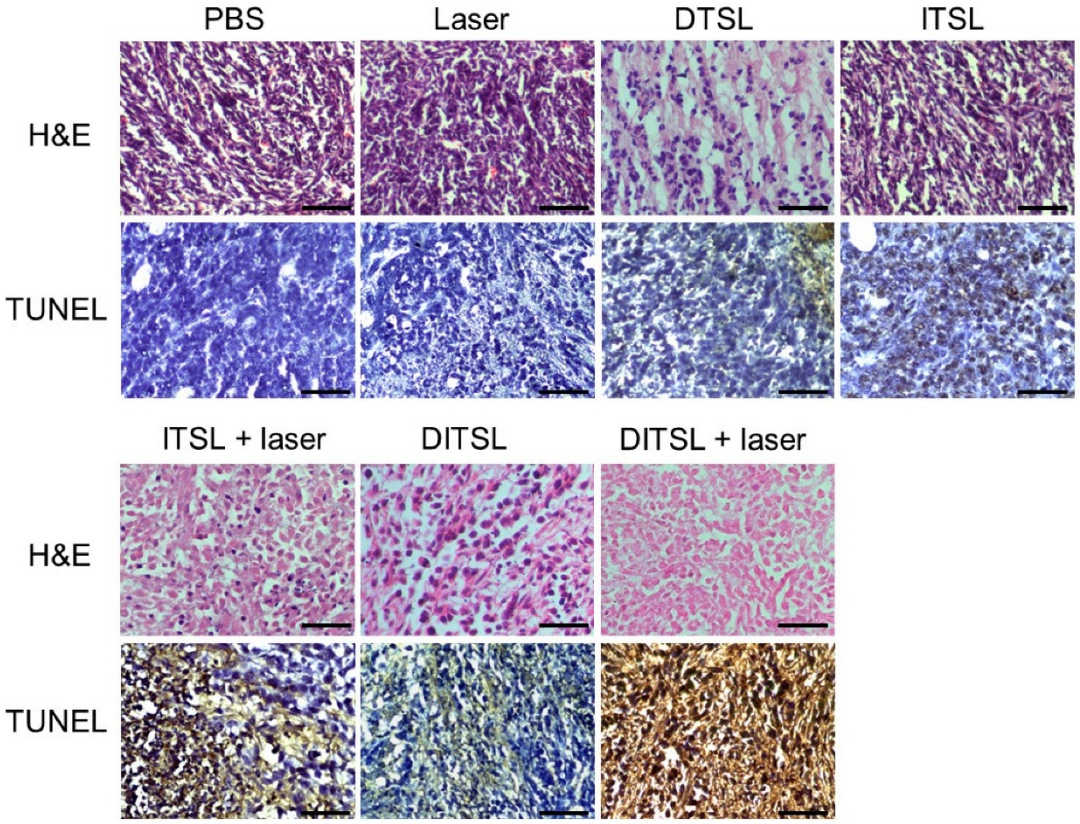

Figure 7. H&E and TUNEL staining. H&E staining and TUNEL staining of non-treated or treated tumors after 48 h. The apoptotic cells were stained in brown by TUNEL assay. Scale bar = 25 μm.

(Fig. 8A and 8C, P<0.01), which were correlated with ultrasonographic examinations. It is easily understood that the coagulative necrosis from PTT would destruct the tumor blood vessels and block the blood perfusion of tumors, resulting in a low or no CEUS signals in the tumor tissues. The larger defective areas in the DITSL + laser-treated tumors could rationally contribute to the combinational effect of chemo-photothermal therapy. In fact, evidences have demonstrated the DOX may play an apparent inhibition role in tumor angiogenesis [49, 50].

Conclusions

In this study, we developed a DOX/IR-780-loaded temperature-sensitive-liposomes (DITSL) to combine PTT with chemotherapeutic agents. Taking advantage of photothermal conversion of IR-780 encapsulated in the shell of liposomes, tumor local high temperature could be induced under NIR-laser irradiation. The local hyperthermia not only produce tumor coagulative necrosis at the central zone above 50°C, but also destruct the shell of temperature-sensitive-liposomes which results in DOX release from the DITSL at peripheral or transitional zone in which the tumor temperature was between 41°C and 45°C. The highly effective chemo-photothermal combination therapy via DITSL greatly improved the anti-tumor efficacy. More importantly, the smart nano-drug platform may achieve NIR-laser-controlled drug release. In conclusion, our study provides a promising strategy to realize synergic chemo-photothermal combination therapy of tumors.

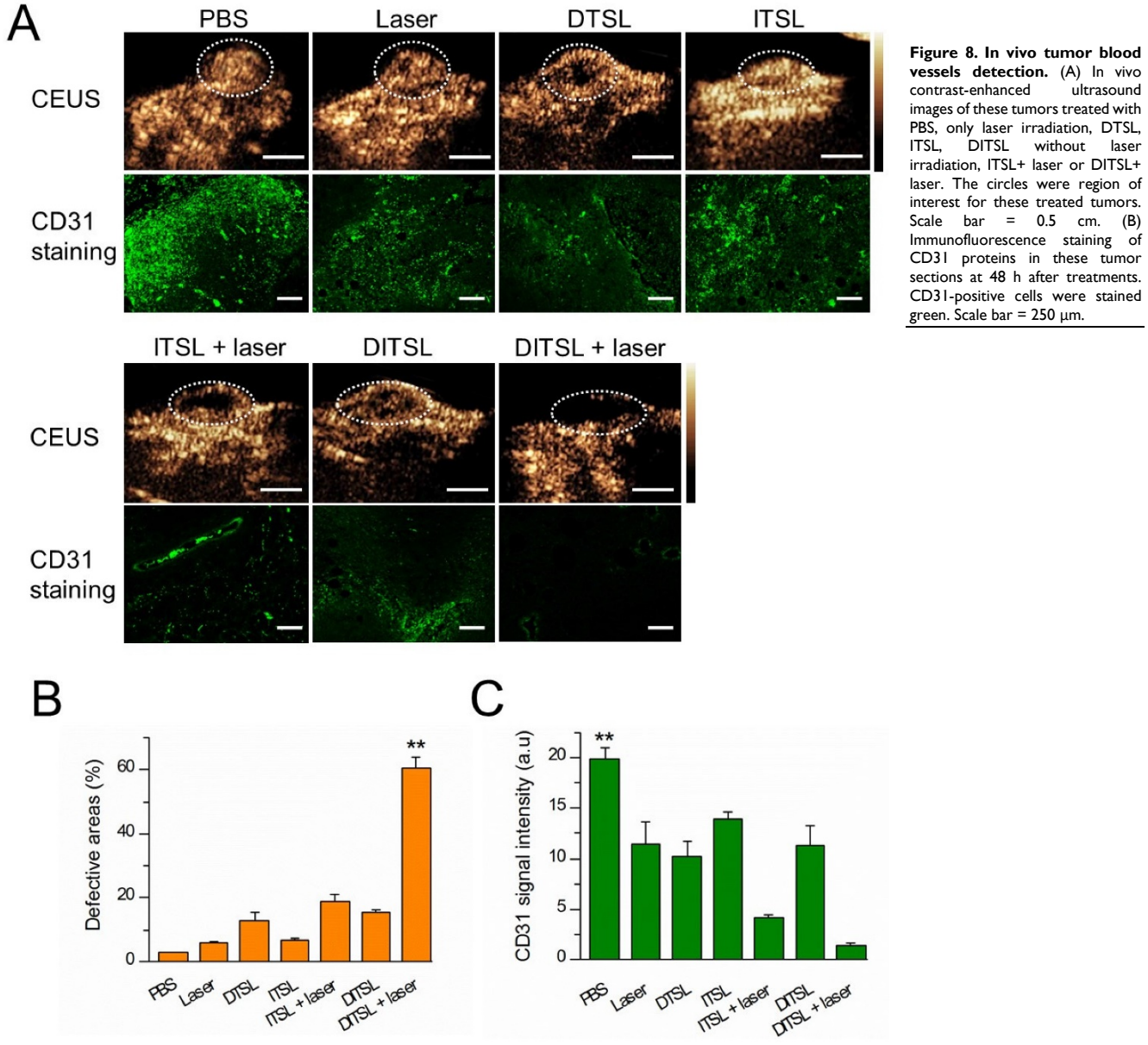

Figure 8. In vivo tumor blood vessels detection. (A) In vivo contrast-enhanced ultrasound images of these tumors treated with PBS, only laser irradiation, DTSL, ITSL, DITSL without laser irradiation, ITSL+ laser or DITSL+ laser. The circles were region of interest for these treated tumors. Scale bar = 0.5 cm. (B) Immunofluorescence staining of CD31 proteins in these tumor sections at 48 h after treatments. CD31-positive cells were stained green. Scale bar = 250 μm.

Supplementary Material

Supplementary figures.
http://www.thno.org/v06p2337s1.pdf

Acknowledgements

The work was supported by National Key Basic Research Program of China (973 Program) (Grant Nos. 2015CB755500, 2014CB744502, 2013CB733800), National Natural Science Foundation of China (Grant Nos. 81571701, 81371563, 81527901, 81430038, 81301242, 11325420, 11534013), Military Medical Scientific Research Plan Project (CWS12J076), Guangdong Provincial Science and Technology Projects (2011B080701019, 2012B031800309, 2014A020212255), Cross-disciplinary Collaborative Teams Program for Science, Technology and Innovation of Chinese Academy of Science, Shenzhen Science and Technology Innovation Committee grants: JCYJ20150521144321010, JCYJ20120617114912864, JCYJ20130401105615484 and ZDSYS20140509162754023.

Competing interests

All the authors declare they have no competing of interests.

References

1. Shibu ES, Hamada M, Murase N, Biju V. Nanomaterials formulations for photothermal and photodynamic therapy of cancer. J Photoch Photobio C. 2013;15: 53-72.
2. Wang Y, Xiao Y, Tang R. Spindle-like polypyrrole hollow nanocapsules as multifunctional platforms for highly effective chemo-photothermal combination therapy of cancer cells in vivo. Chemistry. 2014;20: 11826-34.
3. You J, Zhang R, Xiong C, et al. Effective photothermal chemotherapy using doxorubicin-loaded gold nanospheres that target EphB4 receptors in tumors. Can Res. 2012; 72: 4777-86.
4. Poulose AC, Veeranarayanan S, Mohamed MS, et al. Multi-stimuli responsive Cu2S nanocrystals as trimodal imaging and synergistic chemo-photothermal therapy agents. Nanoscale. 2015;7: 8378-88.
5. Zhang Z, Wang J, Chen C. Near-infrared light-mediated nanoplatforms for cancer thermo-chemotherapy and optical imaging. Adv Mater. 2013; 25: 3869-80.
6. Zhang W, Guo Z, Huang D, et al. Synergistic effect of chemo-photothermal therapy using PEGylated graphene oxide. Biomaterials. 2011; 32: 8555-61.
7. Peralta DV, Heidari Z, Dash S, et al. Hybrid paclitaxel and gold nanorod-loaded human serum albumin nanoparticles for simultaneous chemotherapeutic and photothermal therapy on 4T1 breast cancer cells. ACS Appl Mater Inter. 2015; 7: 7101-11.
8. Tao Y, Ju E, Liu Z, et al. Engineered, self-assembled near-infrared photothermal agents for combined tumor immunotherapy and chemo-photothermal therapy. Biomaterials. 2014; 35: 6646-56.
9. Kim H, Kang J, Chang JH. Thermal therapeutic method for selective treatment of deep-lying tissue by combining laser and high-intensity focused ultrasound energy. Opt Lett. 2014; 39: 2806-9.
10. Wang C, Xu L, Liang C, et al. Immunological responses triggered by photothermal therapy with carbon nanotubes in combination with anti-CTLA-4 therapy to inhibit cancer metastasis. Adv Mater. 2014; 26: 8154-62.
11. Zheng M, Yue C, Ma Y, et al. Single-step assembly of DOX/ICG loaded lipid--polymer nanoparticles for highly effective chemo-photothermal combination therapy. ACS Nano. 2013;7: 2056-67.
12. Liao J, Li W, Peng J, et al. Combined cancer photothermal-chemotherapy based on doxorubicin/gold nanorod-loaded polymersomes. Theranostics. 2015; 5: 345-56.
13. Kim HJ, Lee SM, Park KH, et al. Drug-loaded gold/iron/gold plasmonic nanoparticles for magnetic targeted chemo-photothermal treatment of rheumatoid arthritis. Biomaterials. 2015; 61: 95-102.
14. Konig K. Multiphoton microscopy in life sciences. J Microsc. 2000; 200: 83-104.
15. Hauck TS, Jennings TL, Yatsenko T, et al. Enhancing the toxicity of cancer chemotherapeutics with gold nanorod hyperthermia. Adv Mater. 2008; 20: 3832-8.
16. Wang Y, Black KC, Luehmann H, et al. Comparison study of gold nanohexapods, nanorods, and nanocages for photothermal cancer treatment. ACS Nano. 2013; 7: 2068-77.
17. Park H, Yang J, Lee J, et al. Multifunctional nanoparticles for combined doxorubicin and photothermal treatments. ACS nano. 2009; 3: 2919-26.
18. Zhou M, Li J, Liang S, et al. CuS Nanodots with ultrahigh efficient renal clearance for positron emission tomography imaging and image-guided photothermal therapy. ACS Nano. 2015; 9:7085-96.
19. Monem AS, Elbialy N, Mohamed N. Mesoporous silica coated gold nanorods loaded doxorubicin for combined chemo-photothermal therapy. Int J Pharm. 2014; 470: 1-7.
20. Chu KF, Dupuy DE. Thermal ablation of tumours: biological mechanisms and advances in therapy. Nat Rev Cancer. 2014; 14: 199-208.
21. Ganta S, Devalapally H, Shahiwala A, et al. A review of stimuli-responsive nanocarriers for drug and gene delivery. J Control Release. 2008; 126: 187-204.
22. Lopez-Noriega A, Ruiz-Hernandez E, Quinlan E, et al. Thermally triggered release of a pro-osteogenic peptide from a functionalized collagen-based scaffold using thermosensitive liposomes. J Control Release. 2014; 187: 158-66.
23. May JP, Li SD. Hyperthermia-induced drug targeting. Expert Opin Drug Deliv. 2013; 10: 511-27.
24. Needham D, Dewhirst MW. The development and testing of a new temperature-sensitive drug delivery system for the treatment of solid tumors. Adv Drug Deliver Rev. 2001; 53: 285-305.
25. Shemesh CS, Moshkelani D, Zhang H. Thermosensitive liposome formulated indocyanine green for near-infrared triggered photodynamic therapy: in vivo evaluation for triple-negative breast cancer. Pharm Res. 2015; 32:1604-14.
26. Guo F, Yu M, Wang J, et al. Smart IR780 Theranostic Nanocarrier for Tumor-Specific Therapy: Hyperthermia-Mediated Bubble-Generating and Folate-Targeted Liposomes. ACS Applied Materials & Interfaces. 2015; 7: 20556-67.
27. de Smet M, Langereis S, van den Bosch S. Temperature-sensitive liposomes for doxorubicin delivery under MRI guidance. J Control Release. 2010; 143: 120-7.
28. Yue C, Liu P, Zheng M, et al. IR-780 dye loaded tumor targeting theranostic nanoparticles for NIR imaging and photothermal therapy. Biomaterials. 2013; 34: 6853-61.
29. Park SM, Kim MS, Park SJ, et al. Novel temperature-triggered liposome with high stability: formulation, in vitro evaluation, and in vivo study combined with high-intensity focused ultrasound (HIFU). J Control Release. 2013; 170: 373-9.
30. Kim MS, Lee DW, Park K, et al. Temperature-triggered tumor-specific delivery of anticancer agents by cRGD-conjugated thermosensitive liposomes. Colloid Surface B. 2014; 116: 17-25.
31. Jiang C, Cheng H, Yuan A, et al. Hydrophobic IR780 encapsulated in biodegradable human serum albumin nanoparticles for photothermal and photodynamic therapy. Acta Biomater. 2015;14: 61-9.
32. Al-Jamal WT, Al-Ahmady ZS, Kostarelos K. Pharmacokinetics & tissue distribution of temperature-sensitive liposomal doxorubicin in tumor-bearing mice triggered with mild hyperthermia. Biomaterials. 2012; 33: 4608-17.
33. Tagami T, Ernsting MJ, Li SD. Efficient tumor regression by a single and low dose treatment with a novel and enhanced formulation of thermosensitive liposomal doxorubicin. J Control Release. 2011; 152: 303-9.
34. Banno B, Ickenstein LM, Chiu GN, et al. The functional roles of poly(ethylene glycol)-lipid and lysolipid in the drug retention and release from lysolipid-containing thermosensitive liposomes in vitro and in vivo. J pharm sci. 2010; 99: 2295-308.
35. Dickson JA, Calderwood SK. Temperature range and selective sensitivity of tumors to hyperthermia: a critical review. Ann N Y Acad Sci. 1980; 335: 180-205.
36. Nikfarjam M, Muralidharan V, Christophi C. Mechanisms of focal heat destruction of liver tumors. J Surg Res. 2005; 127: 208-23.
37. Qiu Y, Park K. Environment-sensitive hydrogels for drug delivery. Adv Drug Deliver Rev. 2001; 53: 321-39.
38. Deng Z, Zhen Z, Hu X, et al. Hollow chitosan–silica nanospheres as pH-sensitive targeted delivery carriers in breast cancer therapy. Biomaterials. 2011; 32: 4976-86.
39. Yatvin MB, Weinstein JN, Dennis WH, et al. Design of liposomes for enhanced local release of drugs by hyperthermia. Science. 1978; 202: 1290-3.
40. Shanmugam V, Selvakumar S, Yeh CS. Near-infrared light-responsive nanomaterials in cancer therapeutics. Chem Soc Rev. 2014; 43: 6254-87.
41. Kim H, Jeong SM, Park JW. Electrical switching between vesicles and micelles via redox-responsive self-assembly of amphiphilic rod-coils. J Am Chem Soc. 2011; 133: 5206-9.
42. Chen KJ, Liang HF, Chen HL, et al. A thermoresponsive bubble-generating liposomal system for triggering localized extracellular drug delivery. ACS nano. 2013; 7: 438-46.
43. Tang Y, Lei T, Manchanda R, et al. Simultaneous delivery of chemotherapeutic and thermal-optical agents to cancer cells by a polymeric (PLGA) nanocarrier: an in vitro study. Pharm Res. 2010; 27: 2242-53.
44. Wang Y, Liu T, Zhang E, et al. Preferential accumulation of the near infrared heptamethine dye IR-780 in the mitochondria of drug-resistant lung cancer cells. Biomaterials. 2014; 35: 4116-24.

45. Lagadinou ED, Sach A, Callahan K, et al. BCL-2 inhibition targets oxidative phosphorylation and selectively eradicates quiescent human leukemia stem cells. Cell Stem Cell. 2013;12: 329-41.
46. Peng CL, Shih YH, Lee PC et al. Multimodal image-guided photothermal therapy mediated by 188Re-labeled micelles containing a cyanine-type photosensitizer. ACS Nano. 2011; 5: 5594-607.
47. Hirsch LR, Stafford RJ, Bankson JA, et al. Nanoshell-mediated near-infrared thermal therapy of tumors under magnetic resonance guidance. Proc Natl Acad Sci USA. 2003; 100: 13549-54.
48. Anyarambhatla GR, Needham D. Enhancement of the Phase Transition Permeability of DPPC Liposomes by Incorporation of MPPC: A New Temperature-Sensitive Liposome for use with Mild Hyperthermia. J Liposome Res. 1999; 9: 491-506.
49. Wang K, Zhang X, Liu Y, et al. Tumor penetrability and anti-angiogenesis using iRGD-mediated delivery of doxorubicin-polymer conjugates. Biomaterials. 2014; 35: 8735-47.
50. Al-Jamal KT, Al-Jamal WT, Wang JTW, et al. Cationic poly-l-lysine dendrimer complexes doxorubicin and delays tumor growth in vitro and in vivo. ACS nano. 2013; 7: 1905-17.